Gravity draining of a yield-stress fluid through an orifice

Tim Toplak[a], H. Tabuteau[a], John R. de Bruyn[a], P. Coussot[b],*

[a]*Department of Physics and Astronomy, The University of Western Ontario, London, Ont., Canada N6K 3A7*
[b]*Institut Navier, Université Paris-Est, LMSGC, 2 Allée Kepler, 77420, Champs, France*

Abstract

We study the draining of a yield-stress fluid from a vertical vessel having a hole or a tube at its bottom. In order to understand the basic process we first study the problem with a Newtonian fluid and show that the flow characteristics can be very well described by assuming that the flow is analogous to that through a straight conduit of given length. For a yield-stress fluid draining through a hole the behaviour is different: the flow stops when the pressure drop across the orifice falls to a finite value which increases as the yield stress of the fluid increases or the hole radius R decreases. All the data collapse onto a master curve when plotted in terms of dimensionless numbers involving a characteristic length which is a function of R. We deduce an empirical model for the flow characteristics in such a case. When a length of tube is added after the hole we show that the characteristics of the flow are similar to those for flow through a straight conduit with an equivalent length equal to the tube length plus a fixed additional length.
© 2007 Elsevier Ltd. All rights reserved.

Keywords: Yield-stress fluid; Draining; Extrusion; Orifice

1. Introduction

The drainage or extrusion of pasty materials is widely applied in industry, for example, in the shaping of ceramics, foodstuffs, cosmetics, and other products. In these processes the material is expelled from a large cylinder (the barrel) through a small orifice, under its own weight in the case of drainage, or by an externally applied pressure in the case of extrusion. The control and optimization of this process requires a good knowledge of the flow characteristics of these highly non-Newtonian materials. Despite its wide applicability, however, the state of knowledge in this field is still rather basic. In this paper we focus on the gravity-driven draining of a yield-stress fluid through an orifice at the bottom of a container. This particular type of flow may be encountered in civil engineering when, for example, a volume of concrete, sewage sludge or batter, is emptied from the bottom of a storage hopper. This problem is also related to the flow induced in the so-called "L-Box" test for concrete and the Bostwick consistometer for foodstuffs or paints,

in which a material initially stored in a vertical vessel flows through a gate at the bottom of the vessel. We also expect this work to provide some insight into the extrusion of yield-stress fluids in general.

We note that the word "paste" is used in different fields to describe materials which keep their shape under gravity in the absence of surface tension effects. The expression "yield-stress fluid" is used in rheology to describe a material which exhibits a yield stress but flows as a liquid beyond this yield stress. With these definitions, pastes are similar to yield-stress fluids. Since the stresses induced by gravity increase with sample volume, the yield stress simply defines a critical volume below which the material in a given shape will be unaffected by gravity and beyond which it will be affected. For example, a modelling paste generally keeps its shape under gravity for the small volumes typically used in applications, but would start to flow for much larger volumes. In the following we will use both terms to describe the same systems.

The flow of a fluid through a straight conduit (labelled 1) into another conduit of smaller cross-section (labelled 2) involves some additional viscous dissipation beyond that resulting from the flow in the straight conduits alone. This may be expressed

---

* Corresponding author. Tel.: +33 1 40 43 65 41.
  E-mail address: coussot@lcpc.fr (P. Coussot).

in terms of an additional pressure drop Δp_e, so that the total pressure drop Δp can be written as

$$\Delta p = \Delta p_1 + \Delta p_2 + \Delta p_e. \tag{1}$$

Here Δp_1 and Δp_2 are the pressure drops in the two conduits alone. From the momentum balance in a fluid flowing through a cylindrical conduit of radius R_i and length L_i we get

$$\Delta p_i = (2\tau_{w_i}/R_i)L_i, \tag{2}$$

in which τ_{w_i} is the wall stress in conduit i far from the ends. In some previous work (Boger, 1977) a distinction is drawn between "entrance" and "exit" losses, but here we treat the extra dissipation as a single effect due to the change of cross-section which affects the flow field both before and after the orifice.

For a Newtonian fluid of viscosity μ flowing in steady state in a straight cylindrical conduit, integration of the momentum equation gives the wall stress as

$$\tau_w = 4\mu V/R, \tag{3}$$

where V is the mean flow velocity. In this case, calculations (Sampson, 1891; Hasegawa et al., 1997) for two asymptotic geometries—flow through a conduit of constant radius containing an orifice of negligible thickness, and flow through a long conduit with a stepwise change in radius—led to the expression

$$\Delta p_e = n_e(2\tau_w). \tag{4}$$

n_e is referred to as the entrance correction, and was calculated to be 0.589, while experimental values of n_e range from 0.589 to 1.08 (Boger, 1977). By comparing this result with Eq. (2) it follows that the viscous dissipation due to the change of cross-section is of the same order as the viscous dissipation in a tube of radius R and length L.

The behaviour of yield-stress fluids is described quite well by the Herschel–Bulkley model (Adams et al., 1994, 1997a; Coussot, 2005):

$$\dot{\gamma} = 0 \quad \text{for } \tau < \tau_c$$

and

$$\tau = \tau_c + K\dot{\gamma}^n \quad \text{for } \tau > \tau_c. \tag{5}$$

Here $\dot{\gamma}$ is the shear rate and K and n are material parameters. Let us consider the steady flow of a yield-stress fluid through a tube of length L and radius R. Integration of the expression for the shear rate determined from Eqs. (2) and (5) allows one to derive an expression for the flow rate as a function of pressure drop (Bird et al., 1982). In dimensionless form, this may be written as

$$B_i^{-m} = Y^{-1}(Y-1)^{1+m}\left[1 - \frac{Y^{-1}(1-Y^{-1})}{m+1} - \frac{2(1-Y^{-1})}{m+2}\right], \tag{6}$$

where $Y = R\Delta p/2\tau_c L$, $B_i = \tau_c/K(V/R)^n$, and $m = 1/n$. It is worth noting no flow occurs if the pressure drop is below a critical value equal to $2\tau_c L/R$. Note that this equation assumes no wall slip, an effect which frequently occurs with such pasty materials (Yilmazer and Kalyon, 1989).

Similarly in the case of extrusion of a paste, the existence of the yield stress implies that there should exist a certain critical pressure drop below which no flow is possible. Because the behaviour of such fluids is strongly nonlinear, it is very difficult to find analytical solutions for flows in complex geometries. The entrance correction for the flow of a Bingham fluid (for which the exponent $n = 1$ in Eq. (5)) through an orifice has been determined from numerical simulations to be (Abdali et al., 1992) $n_e = 0.579 + 0.562/\tau_c^*$, where $\tau_c^* = \tau_c R_0/2KV$, R_0 is the radius of the upstream cylinder and V the average velocity through the orifice. Benbow and Bridgwater (1993) modeled extrusion flow of a yield-stress fluid as a homogeneous compression between parallel plates. With this analogy they estimated the minimum die entry pressure drop to be

$$\Delta p_e = \sigma_c \ln(A_0/A), \tag{7}$$

in which σ_c is the uniaxial yield stress (equal to $3^{1/2}\tau_c$, according to Adams et al., 1997b) and A_0 and A are the upstream and downstream cross-sectional areas, respectively. For cylindrical conduits one gets $\Delta p_e = 2\sigma_c \ln(R_0/R)$. Refined expressions involving conical entry angles were determined by Horrobin and Nedderman (1998) from large-deformation elastic–plastic finite element calculations. Benbow and Bridgwater (1993) modified the expression (7) by adding a term depending on V to account for the role of velocity. Alternatively, Basterfield et al. (2005) assumed that the flow through the orifice is equivalent to the flow in a conical duct with an angle around 45° and for cylindrical conduits found Δp_e to be given by

$$\Delta p_e = 2\sigma_c \ln\left(\frac{R_0}{R}\right) + k\left(\frac{V}{R}\right)^n(1 - (R/R_0)^{3n}) \tag{8}$$

with $k = (2/3n)1.2^n \times 3^{(n+1)/2}K$. This reduces to Eq. (7) as V approaches zero. Efforts to verify the above formulae experimentally have mainly been concerned with pastes having a very high yield stress (Basterfield et al., 2005), for which it was difficult to determine the rheological parameters separately.

Here we focus on the gravity-driven flow of simple yield-stress fluids through an orifice. There are two fundamental differences between this flow and pressure-driven extrusion through an orifice: first, the pressure increases with depth from the fluid surface to the orifice at the bottom of the container as a result of the weight of the fluid above, and second, the flow just after the orifice is unconstrained so that, in particular, the pressure there is equal to the ambient pressure. In contrast, in conventional extrusion or flow through an orifice the pressure is imposed upstream, far from the orifice, and decreases downstream. However, as discussed below, it is likely that some characteristics observed here can be extrapolated to conventional extrusion. We first establish a baseline by studying gravity-driven drainage with a viscous Newtonian fluid, then focus on the flow of a yield-stress fluid whose rheological

properties have been well characterised by independent rheometric measurements.

2. Experimental technique and materials

The experimental set up consists of a vertical Plexiglas vessel with a square cross-section of side length W_0. The bottom plate of the vessel has a thickness $e = 4.6$ mm and a hole of radius R in its centre. For some experiments a tube of length l and inner radius R was used instead of a simple hole. Initially the hole is blocked with a piece of tape. The vessel is filled with the experimental fluid, after which the hole is opened so that the fluid can flow out. We monitored the height h as a function of time and shape of the free surface of the fluid as it drained from the vessel with a video camera. Over the course of the experiment the free surface remained approximately flat and horizontal. As the material drained downwards, a thin layer of fluid remained on the vertical walls of the vessel above, implying that slip on the vessel walls was negligible. (The presence of wall slip would imply a finite velocity of the fluid at the wall, so that no material would remain on the wall behind the flow.) The volume of fluid in this layer is small so its effect on the flow rate is negligible and the average downward flow velocity $V_0 = \mathrm{d}h/\mathrm{d}t = \dot{h}$.

Two different types of fluid were used in the experiments. First, we used Newtonian glycerol–water solutions with concentrations of 99% and 90% glycerol by volume. These solutions had densities of 1258 and 1235 kg/m^3, and viscosities at 21 °C of 1.32 and 0.22 Pa s, respectively. We also used two aqueous suspensions of Carbopol ETD 2050 (Noveon). Carbopol is a commercial product based on cross-linked linear polyacrylic acid chains and is commonly used as a thickener. Carbopol gels have a yield stress that depends on concentration and pH due to the existence of a continuous network of micron-sized hydrogel particles throughout the fluid (Carnali and Naser, 1992). They have stable properties and are transparent, making them useful as model yield-stress fluids. Carbopol powder was added slowly to continuously stirred, deionized water to concentrations ϕ of 0.5% and 1.2% by weight. Sodium hydroxide solution was then added to raise the pH to 6. The suspension was further mixed with a propeller-blade mixer at 300 rpm for 10 days, which removed bubbles and homogeneized the material (Tabuteau et al., 2007). The density of both gels was estimated to be 1000 kg/m^3 to within 0.5%.

We determined the rheological properties of the Carbopol gels using a strain-controlled rheometer with a Couette geometry. The measured flow curves are shown in Fig. 1. A steady shear rate was imposed for 15 s and the shear stress measured, starting at high shear rates and working downwards. Since the surfaces of the Couette cylinders were smooth, wall slip is significant at low shear rates (Bertola et al., 2003), as is seen in Fig. 1 for $\dot{\gamma} \leq 0.1\,\mathrm{s}^{-1}$. Ignoring the data in this region, we simply fitted a Herschel–Bulkley model (Eq. (5)) to the data for shear rates larger than $0.1\,\mathrm{s}^{-1}$ as shown in Fig. 1. The fits give $\tau_c = 5.8$ Pa, $K = 5$ Pa s^n for $\phi = 0.5\%$ and $\tau_c = 13.9$ Pa, $K = 9.8$ Pa s^n for $\phi = 1.2\%$, with n fixed at 0.5 in both cases.
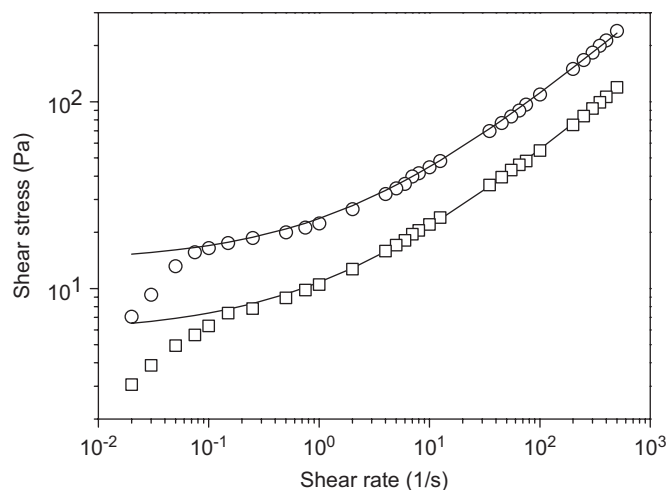

Fig. 1. Flow curves of the two Carbopol gels (squares: $\phi = 0.5\%$; circles: $\phi = 1.2\%$) as measured with a strain-controlled rheometer using a Couette tool. The curves are fits to the Herschel–Bulkley model, Eq. (5), excluding the data at low shear rates for which the effects of wall slip are evident. The fits give $\tau_c = 5.8$ Pa and $K = 5\,\mathrm{s}^{0.5}$ for $\phi = 0.5\%$ and $\tau_c = 13.9$ Pa and $K = 9.8\,\mathrm{s}^{0.5}$ for $\phi = 1.2\%$, with $n = 0.5$ in both cases.

3. Results

3.1. Drainage of a Newtonian fluid

Fig. 2 shows a semi-logarithmic plot of the surface height h as a function of time t for the drainage of the Newtonian glycerol solutions. The height decreases exponentially with time for a range of different hole diameters, vessel sizes and fluid viscosities, deviating from this behaviour at longer times as h approaches zero. The exponential decrease implies that $h \propto \dot{h}$. Since in general the potential energy is proportional to h while viscous effects are proportional to $\dot{h}$, this result suggests that the flow might be described by a balance between potential energy and viscous dissipation, and we thus propose a simple model of the process based on such a balance. We assume that the pressure in the vessel is hydrostatic, i.e., the pressure p at a depth y from the free surface is given by $p = p_0 + \rho g y$, where p_0 is the ambient (atmospheric) pressure. This assumption would be strictly valid for a fluid at rest in a vessel. In our case we approximate the pressure near the entrance to the hole by $p_0 + \rho g h$ and assume that p decreases from this value to p_0 at the exit from the hole, so that the flow occurs as a result of a pressure drop $\Delta p = \rho g h$ across the hole. We model the hole as a cylindrical tube of radius equal to the actual hole radius R and effective length L_e. L_e may differ from the actual hole thickness e due to the approximations made, and may in general depend on the fluid viscosity and the ratio W_0/R. This description is somewhat similar to that for classical extrusion described above.

From Eqs. (2) and (3) above we get

$$\rho g h = \frac{8\mu V L_e}{R^2}, \tag{9}$$

where V is the mean velocity through the orifice. By conservation of mass V may be written as

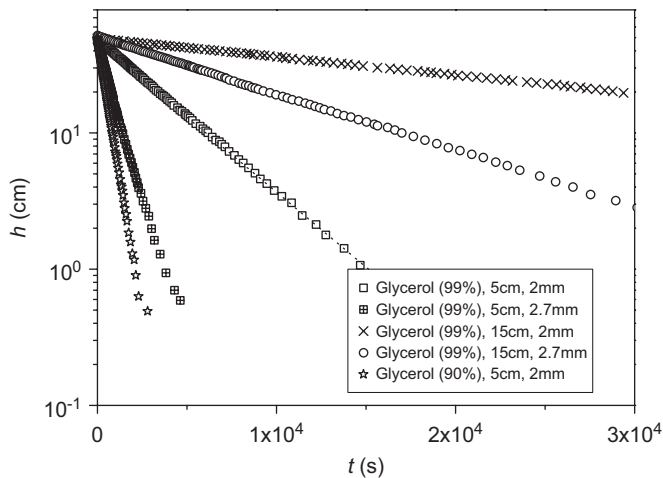$$V = \dot{h} W_0^2 / \pi R^2, \tag{10}$$

Fig. 2. Fluid height h as a function of time for the drainage of the glycerol solutions with a variety of different flow geometries. The different symbols represent different values of W_0 and R, as indicated in the legend.
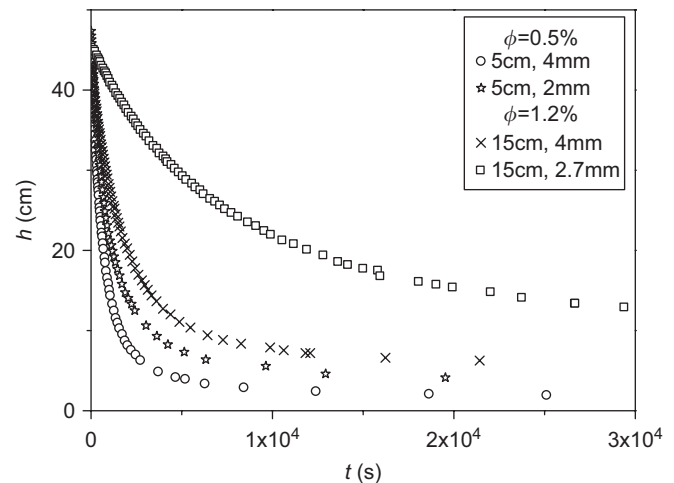

Fig. 4. Height as a function of time for the drainage of Carbopol gels through an orifice, and different flow geometries. The different symbols represent different values of W_0 and R, as indicated in the legend.
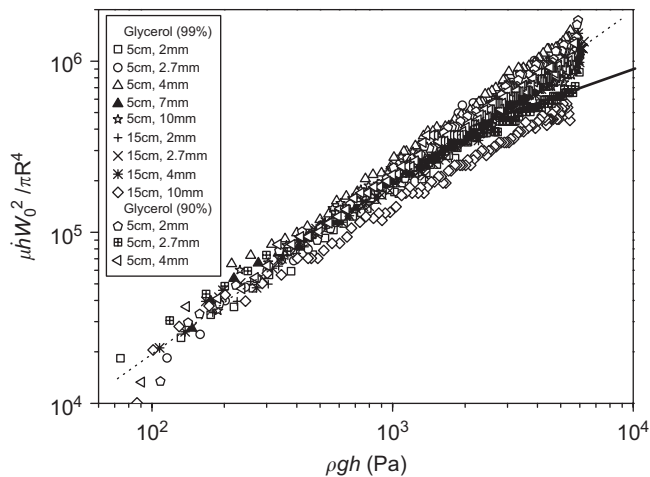

Fig. 3. The glycerol data plotted as $\mu \dot{h} W_0^2 / \pi R^4$ vs. $\rho g h$ for different viscosities and geometric parameters. The dotted line has a logarithmic slope of 1, while the solid line has slope $\frac{1}{2}$. The different symbols represent different values of W_0 and R, as indicated in the legend.

so

$$\rho g h = \frac{8 \mu \dot{h} W_0^2 L_e}{\pi R^4}. \qquad (11)$$

We plot $\rho g h$ as a function of $\mu \dot{h} W_0^2 / \pi R^4$ in Fig. 3. The data from runs for many different conditions collapse within $\pm 10\%$ to a single straight line at low velocities, indicating that this approach is valid and that in fact L_e is independent of W_0 and μ over the range of parameters covered here. A fit gives $L_e = 4.6 \pm 0.2$ mm, which is equal to e within experimental uncertainties, suggesting that one may use the actual thickness of the hole as the effective tube length.

At large flow velocities the data sets for the largest hole diameters and lowest viscosity depart from the straight line found for the other data as described above. For these data the

Reynolds number $R_e = \rho V R / \mu$ is of the order of or larger than 100, suggesting that this deviation is due to inertial effects. For well-developed turbulent flows through an orifice of negligible thickness the inertial term in the momentum equation becomes dominant so that the pressure drop will be given by $\rho g h = \rho V^2$. Using Eq. (10) we see that $\rho g h$ becomes equal to $(\mu \dot{h} W_0^2 / \pi R^4)^2 \rho R^4 / \mu^2$ in this case. This is consistent with the high R_e data plotted in Fig. 3, which appear to tend to a straight line of slope 1/2.

3.2. Drainage of a paste

The height as a function of time for drainage experiments with yield-stress fluids is shown in Fig. 4. In contrast to the results for the Newtonian case, here h does not decrease exponentially: the semi-logarithmic plots are curved and tend to a nonzero height at long times. This height increases with the yield stress τ_c and decreases with the hole radius R. One would expect the flow to stop when the pressure at the entrance to the orifice, i.e., $\rho g h$, is no longer sufficient to overcome the minimum die entry pressure Δp_e. According to Eq. (7), this minimum pressure should increase with τ_c and decrease with R for a fixed value of W_0, as observed.

We will start by assuming that the drainage of the pastes through the orifice can be described using an approach similar to that used for Newtonian fluids above, that is, we again treat the flow as equivalent to that through a tube of radius R and a constant effective length L_e due to a pressure drop Δp equal to the hydrostatic pressure $\rho g h$. If this model was valid, the data plotted as B_i^{-1} vs. Y would fall along a single curve given by Eq. (6). In fact this is not the case: for fixed L_e, our data do not collapse and have a shape different from that of Eq. (6). The data do collapse, however, if we treat L_e as an adjustable parameter in the calculation of an effective value of Y, which we refer to as Y_e, and plot B_i^{-1} as a function of Y_e. The result is shown in Fig. 5. The master curve through the data can be
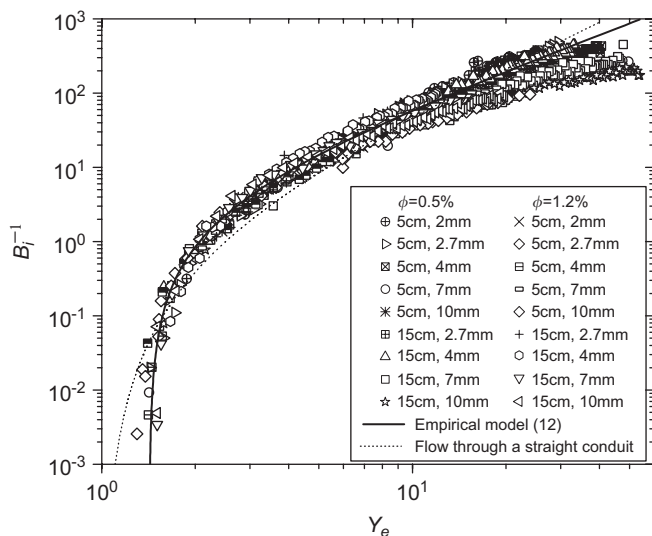
Fig. 5. Flow characteristics for the drainage of Carbopol through an orifice, plotted in dimensionless form as B_i^{-1} vs. Y_e as described in the text. The dashed line is a curve given by Eq. (6) and the solid line is the model given by Eq. (12). The different symbols represent different values of W_0 and R, as indicated in the legend.
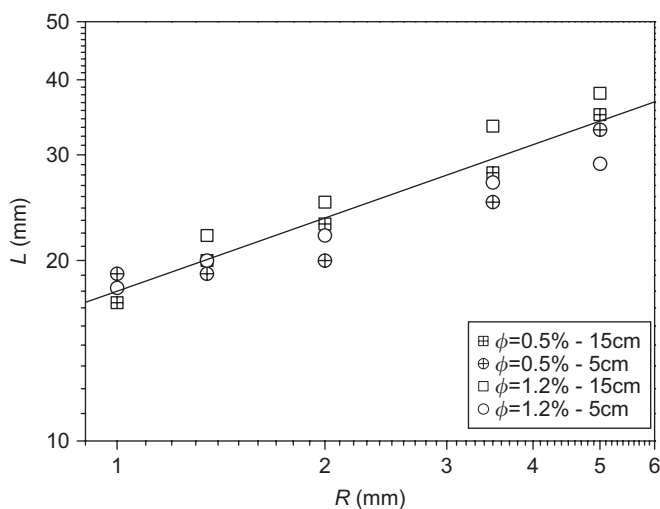

Fig. 6. The characteristic length L_e used to collapse the data in Fig. 5 as a function of R for different flow conditions. The solid line corresponds to the empirical model discussed in the text.

described by the empirical equation

$$Y_e = 1.42 + 0.64 B_i^{0.64}, \qquad (12)$$

which is shown as a solid line in Fig. 5. The values of L_e required to collapse the data increase with the hole radius R, as shown in Fig. 6. Within the experimental scatter, we find $L_e = 0.285 R^{0.4}$, with both L_e and R in meters.

It is difficult to generalise our results to values of the dimensionless ratios R/W_0 and R/h outside of the ranges covered by our experiments, since their dependence on these quantities is not obvious. However we note that, in contrast with the prediction of Eq. (7) (Benbow and Bridgwater, 1993) we observe
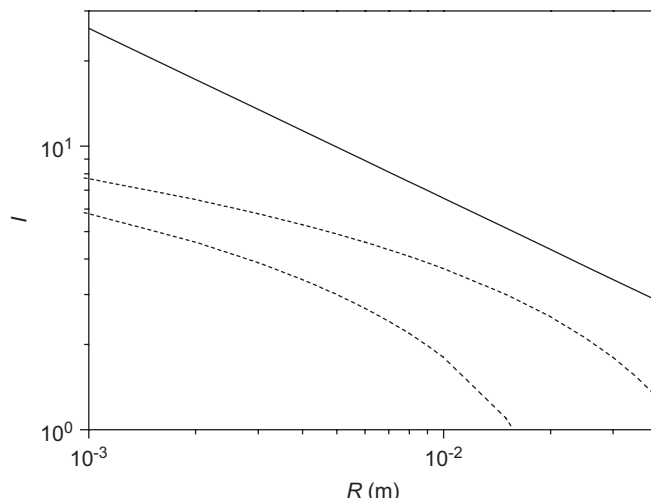

Fig. 7. Comparison of our results (Eq. (12); solid curve) with the predictions of Benbow and Bridgwater (Eq. (7)) for $W_0 = 15$ cm (upper dashed curve) and $W_0 = 5$ cm (lower dashed curve).

no strong dependence on the vessel size. Eq. (12), which was obtained from the master curve fit to the data plotted in Fig. 5, predicts that the flow stops for $Y_e = 1.42$. Using the definition of Y_e and the experimentally determined expression for L_e, we define a new dimensionless pressure-drop parameter $I \equiv Y_e L_e / R$ which is equal to $I = \Delta p / 2\tau_c = 1.42 \times 0.285 R^{-0.6} = 0.4 R^{-0.6}$. In contrast, Eq. (7) would predict that $I = \sqrt{3} \ln(W_0/\sqrt{\pi} R)$. In Fig. 7 we plot I as a function of R for our experimental results and as predicted by Eq. (7) for two values of W_0; the latter underestimates the effective pressure drop for small R/W_0 by more than a factor of 2.

Finally, we consider experiments in which the vessel drained through a length l of tubing with radius $R = 1.75$ mm, rather than a simple hole. The data for h as a function of time are qualitatively similar to those plotted in Fig. 4: h decreases non-exponentially with time, there is an asymptotic height at long times which increases with the yield stress of the fluid. We analyse this behaviour using the same model, and calculate Y_e using a total effective length $L_t = L_e + l$, where l is the actual length of the tube and L_e is the effective length of the orifice, as above. B_i^{-1} is plotted as a function of Y for several values of l and W_0 in Fig. 8. A value of $L_e = 22.5$ mm was used to collapse all of the data along a single curve corresponding to Eq. (6). This description is consistent with the above approach for the flow through an orifice alone: it predicts $\rho g h / 2\tau_c = 15.4$ for $l = 4.6$ mm and $V = 0$ ($Y = 1$), which is close to the value of 18.6 found from Eq. (12) for $V = 0$ and $R = 1.75$ mm. Note that the data tend to a horizontal plateau (constant velocity) at low depths (small Y), likely due to wall slip becoming important at low velocities.

These results show that Eq. (6) provides a good representation of the data when the yield-stress fluid drains through a tube of length larger than the orifice diameter, but not when there is no tube present. Further insight into the origin of this behaviour could be gained from local measurements of the velocity field using, for example, particle image velocimetry.
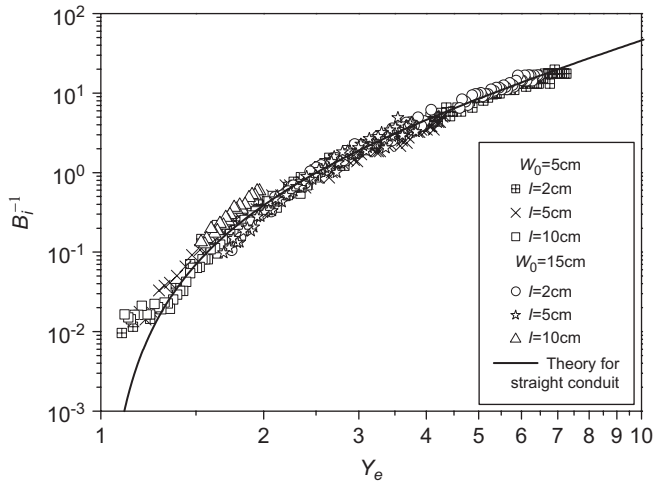
Fig. 8. Flow characteristics for the drainage of Carbopol gels through an orifice followed by a tube for different flow geometries. The data are plotted in dimensionless form as B_i^{-1} vs. Y_e, taking into account a dependence of L_e on the tube length, as discussed in the text. The different symbols represent different values of W_0 and R, as indicated in the legend.

4. Conclusion

Our results provide an expression for the critical pressure drop associated with the stoppage of flow in the drainage, and by extension in the extrusion, of yield-stress fluids. We find

$$\Delta p = \rho g h = 2\tau_c \frac{C}{R},$$

where $C = 0.4R^{0.4}$ when the downstream length l is small (on the order of R) and $C = l + l_0$ when l is much larger than R. In developing these expressions from our data, we have assumed that the viscous dissipation in our flows was analogous to that for shear flow through a tube. The application of these results to conventional extrusion flows remains to be confirmed experimentally.

Notation

A_0, A	upstream and downstream cross-sectional areas
B_i	Bingham parameter: ratio of the yield stress to the viscous stress
e	thickness of the vessel bottom plate
g	acceleration due to gravity
h	fluid height in the vessel
I	dimensionless pressure parameter
K, n	parameters of the Herschel–Bulkley model
l	length of the additional downstream tube
L	conduit length
L_e	length of the tube leading to a pressure drop Δp_e
$m = 1/n$	
n_e	entrance correction
p	pressure
p_0	ambient pressure
Δp	pressure drop
Δp_e	pressure drop due to a change in cross-section
R	radius of the vessel orifice, or of the downstream conduit
R_e	Reynolds number
R_0	radius of the upstream conduit
V	mean flow velocity
V_0	mean fluid velocity in the vertical direction in the vessel
W_0	vessel side width
Y	dimensionless pressure drop

Greek letters

$\dot{\gamma}$	shear rate
μ	Newtonian fluid viscosity
ρ	fluid density
σ_c	uniaxial yield stress
τ	shear stress
τ_c	yield stress
τ_w	wall stress
φ	Carbopol concentration

References

Abdali, S.S., Mitsoulis, E., Markatos, N.C., 1992. Entry and exit flows of Bingham fluids. Journal of Rheology 36, 389–407.
Adams, M.J., Edmonson, B., Caughey, D.G., Yahya, R., 1994. An experimental and theoretical study of the squeeze-film deformation and flow of elastoplastic fluids. Journal of Non-Newtonian Fluid Mechanics 51, 61–78.
Adams, M.J., Briscoe, B.J., Corfield, G.M., Lawrence, C.J., Papathanasiou, T.D., 1997a. An analysis of the plane-strain compression of viscoplastic materials. Journal of Applied Mechanics-Transactions of the ASME Series E 64, 420–424.
Adams, M.J., Aydin, I., Briscoe, B.J., Sinha, S.K., 1997b. A finite element analysis of the squeeze flow of an elasto-plastic paste material. Journal of Non-Newtonian Fluid Mechanics 71, 41–57.
Basterfield, R.A., Lawrence, C.J., Adams, M.J., 2005. On the interpretation of orifice extrusion data for viscoplastic materials. Chemical Engineering Science 60, 2599–2607.
Benbow, J., Bridgwater, J., 1993. Paste Flow and Extrusion. Clarendon Press, Oxford.
Bertola, V., Bertrand, F., Tabuteau, H., Bonn, D., Coussot, P., 2003. Wall slip and yielding in pasty materials. Journal of Rheology 47–61, 1211.
Bird, R.B., Gance, D., Yarusso, B.J., 1982. The rheology and flow of viscoplastic materials. Review in Chemical Engineering 1, 1–70.
Boger, D.V., 1977. Separation of elastic and shear thinning effects in the capillary rheometer. Transactions of the Society of Rheology 21, 515–534.
Carnali, J.O., Naser, M.S., 1992. The use of dilute solution viscosimetry to characterize the network properties of carbopol microgels. Colloid Polymer Science 270, 183–193.
Coussot, P., 2005. Rheometry of Pastes, Suspensions and Granular Materials. Wiley, New York.
Hasegawa, T., Suganuma, M., Watanabe, H., 1997. Anomaly of excess pressure drops of the flow through very small orifices. Physics of Fluids 9, 1–3.
Horrobin, D.J., Nedderman, R.M., 1998. Die entry pressure drops in paste extrusion. Chemical Engineering Science 53, 3215–3225.
Sampson, R.A., 1891. On Stokes's current function. Philosophical Transactions of the Royal Society of London Series A 182, 449.
Tabuteau, H., Coussot, P., de Bruyn, J.R., 2007. Drag force on a sphere in steady motion through a yield-stress fluid. Journal of Rheology 51, 125–137.
Yilmazer, U., Kalyon, D.M., 1989. Slip effects in capillary and parallel disk torsional flows of highly filled suspensions. Journal of Rheology 33, 1197–1212.